

CONTRIBUTION OF SEISMIC ATTRIBUTES IN THE DIRECT DETECTION OF HYDROCARBON, CASE HISTORY OF A PERMIT IN THE SOUTH ALGERIAN SAHARA

MabroukDJEDDI*, Jalel FERRAHTIA*, Mounir DJEDDI** et Moh Amokrane AITOUCHE*

ABSTRACT

The zone of interest is located in an important oil and gas zone; its position near Berkine and Illizi basin makes it very important. Our study is based on the data collected on two seismic lines, according to the lines A and B, which intersect on well-2. The present work is based on the study of the contribution of the seismic attributes, in particular the amplitude attribute presented by the AVO method, to the direct hydrocarbons detection. The use of the seismic attributes and above all the AVO method becomes very widespread those latest years. With this study we wanted to show the sturdiness and the supply the additional information that can bring those attributes. We checked, in spite of the very poor quality of the data and the high noise level, that having recours to attributes such as amplitude, frequency and phase yields an invaluable information concerning the nature of the fluid, the continuity of the reflectors, the localisation of the discontinuities etc... ; many anomalies were localised in diverse places along the two profiles ; those anomalies may be used like a mark during the future studies on the region. (Note: due to the confidentiality of the data, authors have kept seismic lines and wells anonymous).

Key Words - AVO - DHI - Hilbert transform - Instantaneous frequency - Instantaneous phase-
INVEST - Seismic attributes.

CONTRIBUTION DES ATTRIBUTS SISMIQUES DANS LA DETECTION DIRECTE DES HYDROCARBURES. APPLICATION SUR UN PERMIS DU SAHARA (SUD ALGERIEN)

RÉSUMÉ

La zone objet de notre étude est localisée dans une région importante au plan pétrolier et gazier en raison de sa position privilégiée par rapport aux bassins de Berkin et d'Illizi. Notre étude repose sur des données sismiques 2D, incluant les lignes A et B traversant le puits 2. Le présent travail est une contribution sur les attributs sismiques, en particulier l'attribut amplitude illustrée par la méthode AVO pour la détection directe des hydrocarbures.

L'application des attributs sismiques et partant de la technique AVO s'imposent de plus en plus au cours de ces dernières années. A travers la présente étude, nous voulons surtout

* Laboratoire de Physique de la Terre Faculté des Hydrocarbures et de la Chimie Université de Boumerdés 35000 ALGERIE

** Laboratoire des systèmes et signaux SUPELEC Plateau du Moulon 91192 Gif sur Yvette France

- Manuscrit déposé le 07 Avril 2001, accepté après révision le 17 Septembre 2002.

montrer toute l'importance à accorder aux attributs sismiques vecteurs d'une information complémentaire. Nous avons voulu, malgré la mauvaise qualité des données sismiques entre autres le niveau de bruit, le recours aux attributs sismiques tels que l'amplitude, la fréquence et la phase caractérisant la nature du fluide, la continuité des réflecteurs, la localisation des discontinuités etc... Plusieurs autres anomalies ont été localisées le long des deux lignes; elles seront considérées comme des éléments de repère pour les futures études sur la même région. Note: le caractère confidentiel des données sismiques ont amené les auteurs à rendre anonymes les lignes sismiques et les puits de référence

Mots clé - AVO - Transformation de Hilbert - Fréquence instantanée - Phase instantanée - Programme INVEST - Attributs sismiques.

INTRODUCTION

We've always observed, during seismic prospecting, signal amplitudes, but our goal was only its existence and not its magnitude, because we were looking for structural forms. Ostrander (1984) was the first to introduce oil and gas reservoirs delimitation using seismic amplitude anomalies by using the AVO method. The amplitude anomaly called "bright spot" was used for many decades as direct hydrocarbon indicator, particularly gas accumulation. Unfortunately, many other factors may produce "false" bright spots as overpressurised geological formations, coal layers, high porosity sands or non commercial gas accumulation. Ostrander's study, linked Poisson's ratio (σ) to gas saturation and then to amplitude variation with offset.

Poisson's ratio (σ) links compressional wave velocity (V_p) and shear wave velocity (V_s) by the following relationship

$$\sigma = \frac{\left(\frac{V_p}{V_s}\right)^2 - 2}{2\left[\left(\frac{V_p}{V_s}\right)^2 - 1\right]} \quad (1)$$

The AVO method principle is to calculate amplitude variation with offset or angle of incidence (AVA) according to variations in petrophysical properties. Generally, an incident compressional wave at a non normal angle produces a phenomenon called "energy"

Table I. AVO response class (after Rutherford and Williams 1989)

Classe de réponses AVO

Class	Reservoir type	AVO response characteristic
Class I	high impedance sands	high value of R_0 with amplitude decrease with offset
Class II	near zero impedance sands	- near zero R_0 value with an increase of amplitude with offset - near zero R_0 value with polarity inversion at intermediate offsets
Class III	very low impedance sands	-strong negative value of R_0 with absolute Amplitude increase with offset

partitioning that gives two kinds of waves, two reflecting waves, compressional and shear waves, and two transmitting waves, compressional and shear waves.

Mathematical equations describing the phenomenon of energy partitioning are called Zoeppritz equations (1919). Because these equations are so complex and not easy to handle, many approximations were set. Among these approximations, the Aki and Richards approximations (1980), the Hilterman approximation (1983), and the Shuey approximation (1985), the latest fits at moderate angles of incidence; the Shuey approximation is given by Thomsen (1993) and A. Rüger (1994) by

$$R_p(\theta) = \frac{1}{2} \frac{\Delta Z}{Z} + \frac{1}{2} \left[\frac{\Delta V_p}{V_p} - \left(\frac{2V_s}{V_p} \right)^2 \frac{\Delta G}{G} \right] \sin^2(\theta) + \frac{1}{2} \left(\frac{\Delta V_p}{V_p} \right) \sin^2(\theta) \tan^2(\theta) \quad (2)$$

with $Z = \rho V_p$ acoustical impedance of P waves,

$G = \rho V_s^2$ shear wave modulus; $\Delta(\bar{\quad})$ and $\bar{\quad}$ are difference and mean values of petrophysical properties respectively (here ρ is the medium density). Another variant of Shuey's approximation introduces Poisson's ratio variations by

$$R_p(\theta) = R_0 + \left[A_0 R_0 + \frac{\Delta \sigma}{(1 - \sigma)^2} \right] \sin^2(\theta) + \frac{1}{2} \frac{\Delta V_p}{V_p} [\tan^2(\theta) - \sin^2(\theta)] \quad (3)$$

where

$$R_0 = \frac{1}{2} \left(\frac{\Delta V_p}{V_p} + \frac{\Delta \rho}{\rho} \right)$$

and

$$A_0 = B - 2(1 + B) \frac{1 - 2\sigma}{1 - \sigma}$$

$$B = \frac{\frac{\Delta V_p}{V_p}}{\frac{\Delta V_p}{V_p} + \frac{\Delta \rho}{\rho}} \quad (4)$$

\bar{V}_p , $\bar{\rho}$, $\bar{\sigma}$ are petrophysical mean values.

Notice that the more the contrast in Poisson's ratio (equation 3) the more important is the AVO response.

By replacing interstitial water in a rock by gas, a remarkable changing in the Poisson's ratio has been measured (Ostrander 1984).

Variations in Poisson's ratio may also be caused by age, compaction or presence of impurities like shale.

Equation (3) can be written as

$$R_p(\theta) = R_0 + AR_0 \sin^2(\theta) \quad (5)$$

The above equation is made up to of two parts: the first includes normal incidence coefficient, the second part includes amplitude variations with angle incidence. Usually call it *gradient* or G , then, by reporting angle incidence values on x axis and amplitude values on y axis, R_0 and G values may be deduced by regression (R_0 is usually called *intercept* and G *gradient*).

Intercept x gradient product (PxG) is a powerful hydrocarbon indicator. By definition, low impedance sands (Rutherford and Williams 1989. Table I gives the AVO response class.

ANALYTICAL TRACE CONCEPT

A seismic trace can be described as real part of complex analytical trace $s(t) = g(t) + js_H(t)$ which is made up of real part and imaginary part. Imaginary part $S_H(t)$ is generated by Hilbert Transform of real trace $S(t)$.

$$TH[s(t)] = s_H(t) = s(t) * \frac{1}{\pi t} \quad (6)$$

(*) represents convolutional product.

Then the analytical complex signal may be written as

$$S(t) = s(t) + js_H(t) \quad (7)$$

where $s(t)$ is the real part, $js_H(t)$ is the imaginary part and $j^2 = -1$.

Seismic amplitude is then square sum of real trace and imaginary part:

$$R(t) = [s(t)^2 + h(t)^2]^{1/2} \quad (8)$$

We also call this sum "instantaneous amplitude". The attribute phase is given by

$$\theta(t) = \tan^{-1} \left[\frac{h(t)}{g(t)} \right] \quad (9)$$

and instantaneous frequency is given by

$$f_{inst} = \frac{\partial \theta(t)}{\partial t} \quad (10)$$

CASE HISTORY

The zone of interest is producing in the upper and lower "triassic shally sandstones" (TAGS, TAGI) and in the Gothlandian.

Triassic sands are interpreted as shallow marine deposits; traps in this region are of two kinds: structural and stratigraphic. Reservoir are located at 2800m depth.

SEISMIC DATA PROCESSING SEQUENCE

One of the most important parameter during a seismic attribute study and in AVO is processing, which may be held to minimum and carried in such a way to preserve relative reflect-

tion amplitudes. Seismic data of this case history are very poor and with a very low fold coverage (1200% for line A and 2400% for line B). The non homogeneity of these conditions drives us to be more careful during processing. Many steps were put aside, as F-K filtering, and the powerful noise suppression, the CDP stack, because we have used the prestack space. As mentioned earlier, the seismic lines were characterized by a high noise level; to eliminate these noises we used a very efficient tool which is the INVEST method (Thomsen 1984). The improvement S/N ratio is evident (see fig. 2, compared with figure 1, which is a portion of stacked seismic section without application of INVEST). Number of other processing steps were used like spherical divergence correction, inelastic attenuation correction and surface consistent real amplitude recovery. Final seismic sections are given in figures (3a and 3b).

AVO Method Results

The most consistent representation used in this study is the product (intercept x gradient); in fact, presence of gas produces a positive anomaly (red colour) (fig. 4). The anomaly in figure 4 is produced near CDP 688 at double time 2320 ms. Positive values are probably due to negative values of intercept and gradient. We have also used the fluid factor representation (Smith and Gildow 1987). The fluid factor is given by.

$$\Delta F = \frac{\Delta V_p}{V_p} - 1.16 \left(\frac{V_s}{V_p} \right) \frac{\Delta V_s}{V_s} \quad (11)$$

with $\Delta V_p/V_p$ and $\Delta V_s/V_s$ fractional velocity variation of P and S wave respectively; 1.16 is a constant proposed by Castagna *and al.*, (1994). The fluid factor gives the difference between $\Delta V_p/V_p$ observed values and those predicted from $\Delta V_s/V_s$. Theoretically, water saturated rocks have zero fluid factor. Figure 5

CONTRIBUTION OF SEISMIC ATTRIBUTES IN THE DIRECT DETECTION OF HYDROCARBON

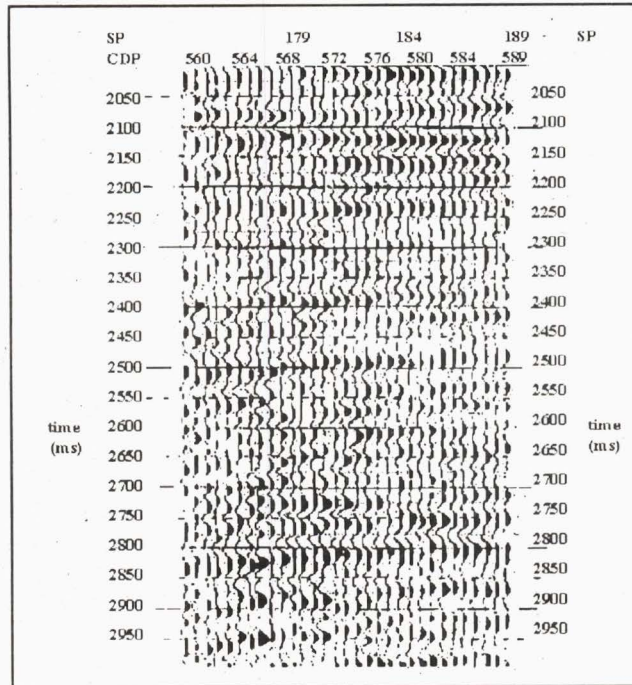


Fig. 1 - Portion of stacked seismic section without application of INVEST

Portion d'une section sismique après sommation mais avant application du programme INVEST

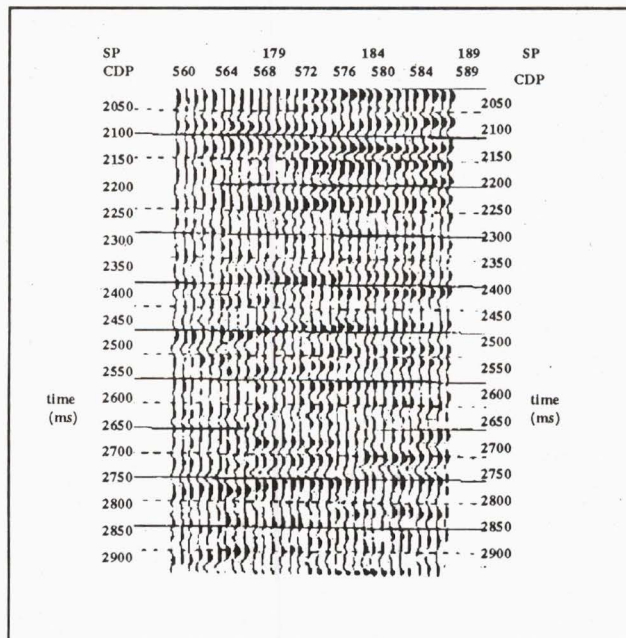


Fig. 2 - Same portion of stacked seismic section with application of Raon transform

Même portion de section sismique après application de la transformation de Radons (INVEST)

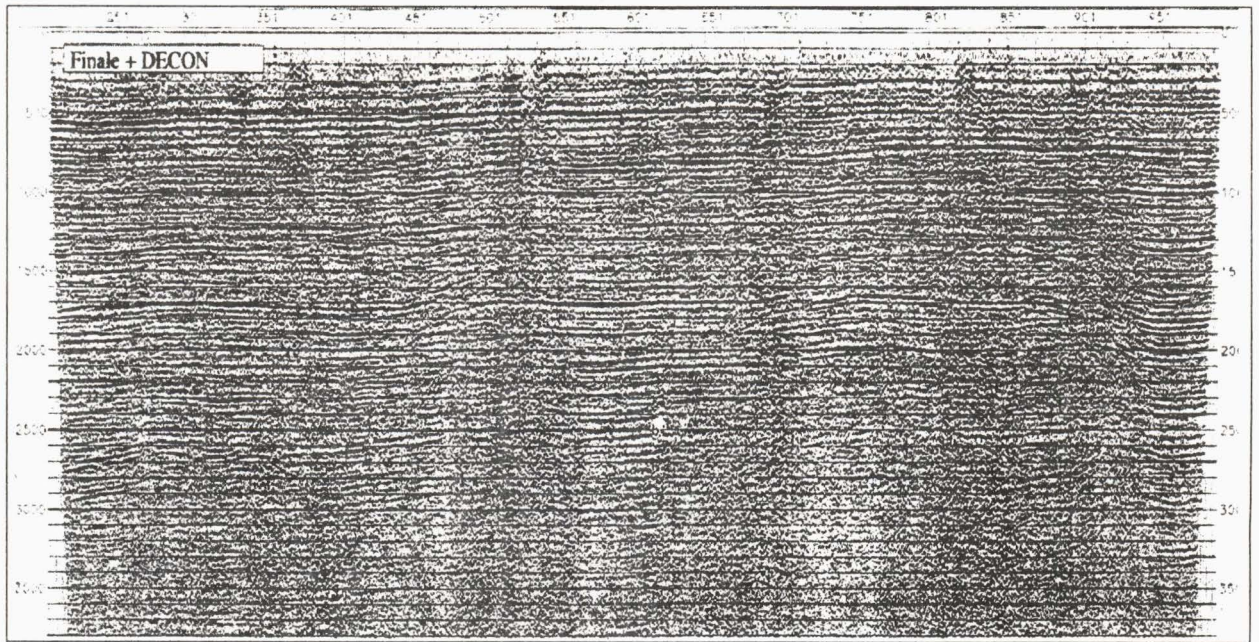


Fig. 3a - Final seismic section of line A
Section sismique finale pour le profil A

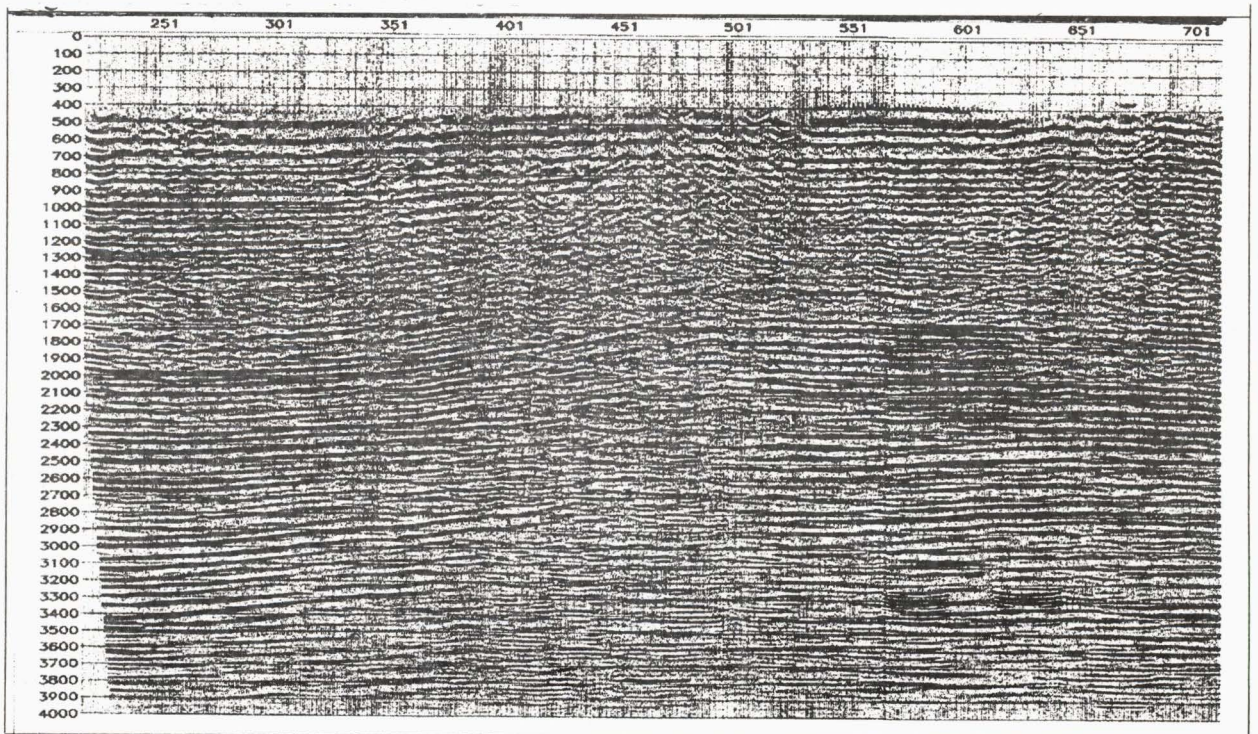


Fig. 3b - Final seismic section of line B
Section sismique finale pour le profil B

CONTRIBUTION OF SEISMIC ATTRIBUTES IN THE DIRECT DETECTION OF HYDROCARBON

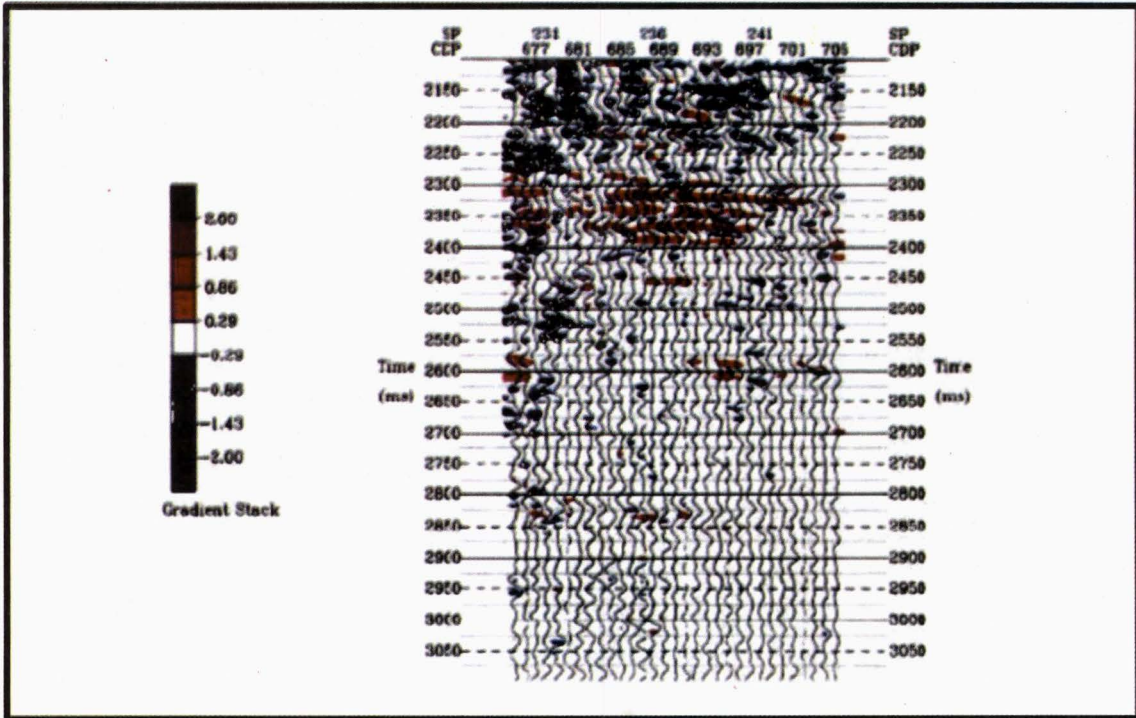


Fig. 4 - P*G representation of anomaly at double time 2300ms near CDP 688
 Représentation P*G pour l'anomalie sise au temps double 2300ms près du CDP 688

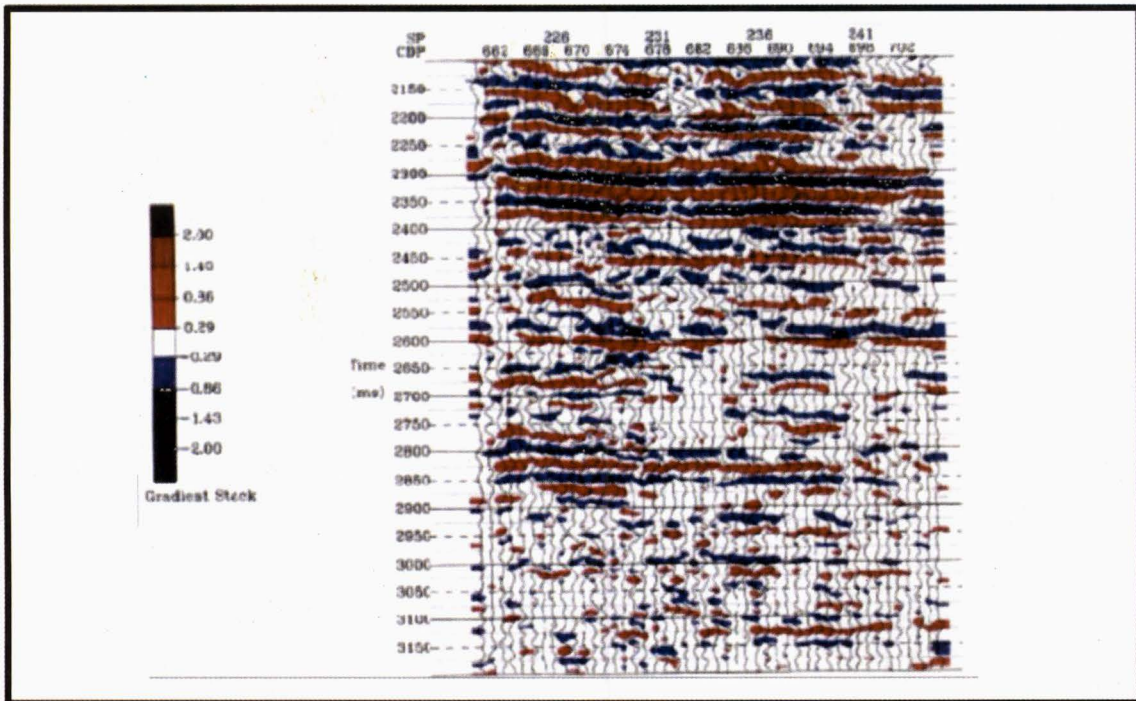


Fig. 5 - Fluid factor representation of figure 4 anomaly
 Représentation en facteur fluide de l'anomalie signalée en figure 4

is a fluid factor representation of anomaly produced near CDP 688 at time 2320ms.

By reporting seismic data in AB plane (intercept, gradient), one can separate anomalies depending on whether intercept and gradient values are positive or negative. The more these values are negative the more they are interesting. Negative values are characteristic of gas sands top. Figure 6 is a representation in AB plane, anomalous zones are marked zone 1 and 2, and they define top and bottom of zone of interest, these zones define anomaly near CDP 688. Notice that line passing through the origin is called fluid line and all values deviating from this line define the so called hydrocarbon line.

SEISMIC ATTRIBUTES RESULTS

Line A anomaly near CDP 388 was displayed on instantaneous phase and frequency. Generally, instantaneous phase representations are useful when we look for discontinuities (fault localisation); the phase being independent of amplitude, strong and peak reflections will have the same appearance. Figure 7 shows a discontinuity near CDP 430 at double time 2600ms; the same discontinuity is not so obvious on classic seismic section. In fact, this zone is directed NE by a fault system in Berkine depression and NNW in Illizi basin. Instantaneous frequency is very sensitive to reflection interference, it is very useful in lithologic and facies determination. Figure 8 shows lateral facies change near CDP 562 at double time 2025ms.

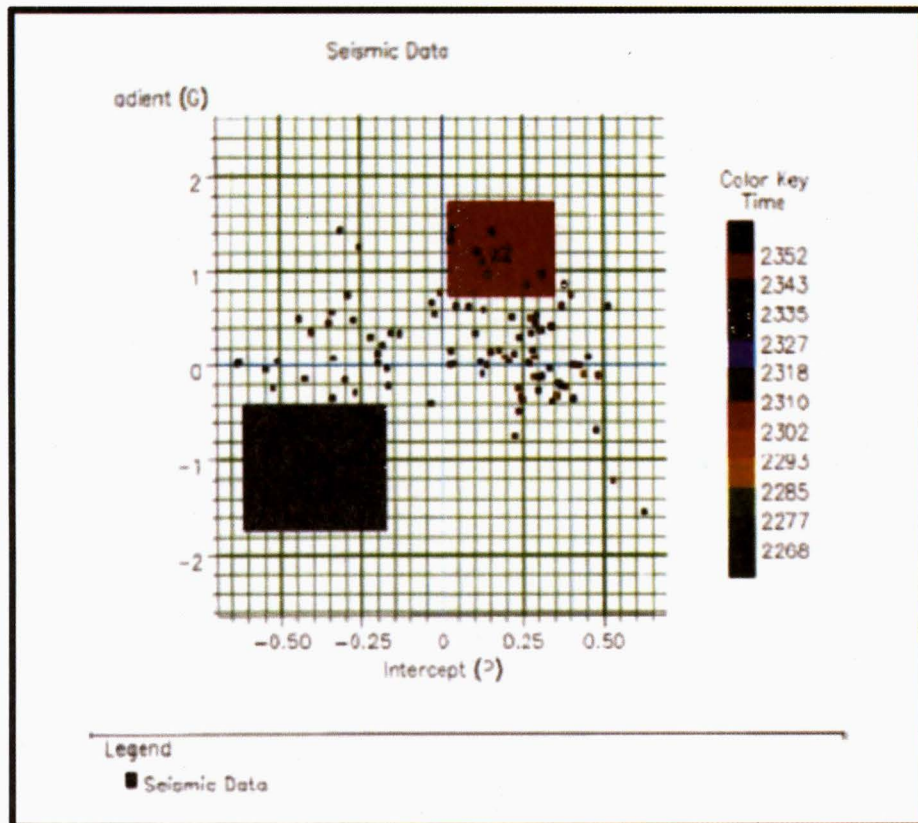


Fig. 6 - Intercept-gradient (AB) plane analysis

Analyse Intercept-Gradient dans le plan (AB)

CONTRIBUTION OF SEISMIC ATTRIBUTES IN THE DIRECT DETECTION OF HYDROCARBON

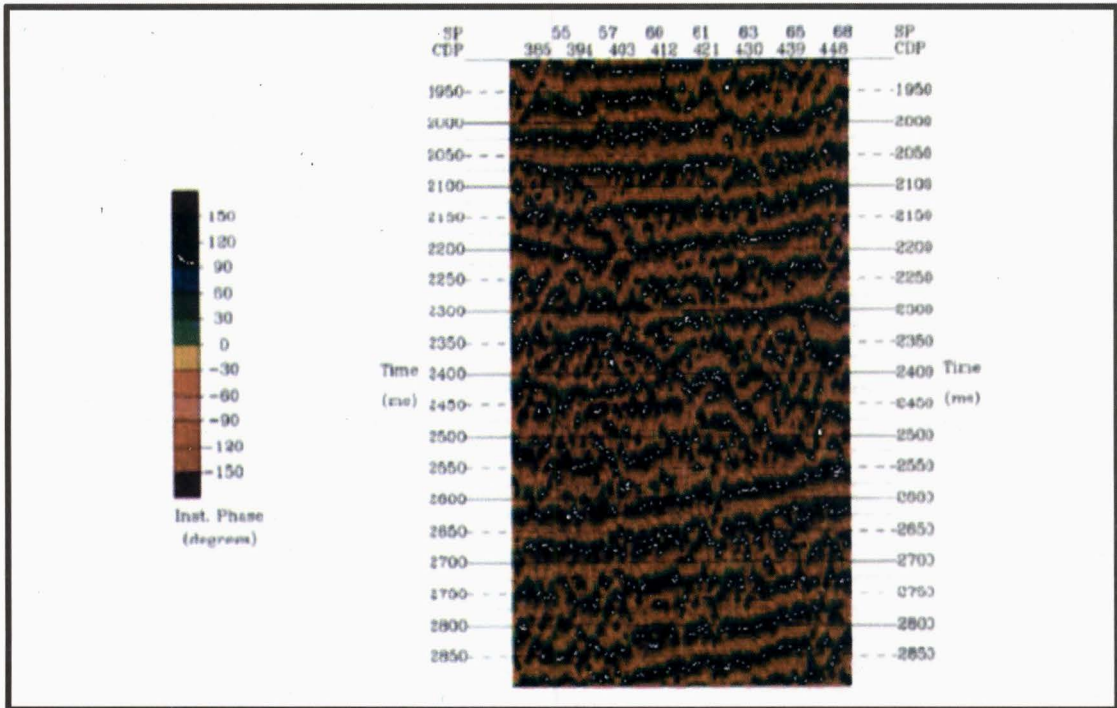


Fig. 7 - Phase attribute representation
Représentation en attribut phase instantanée

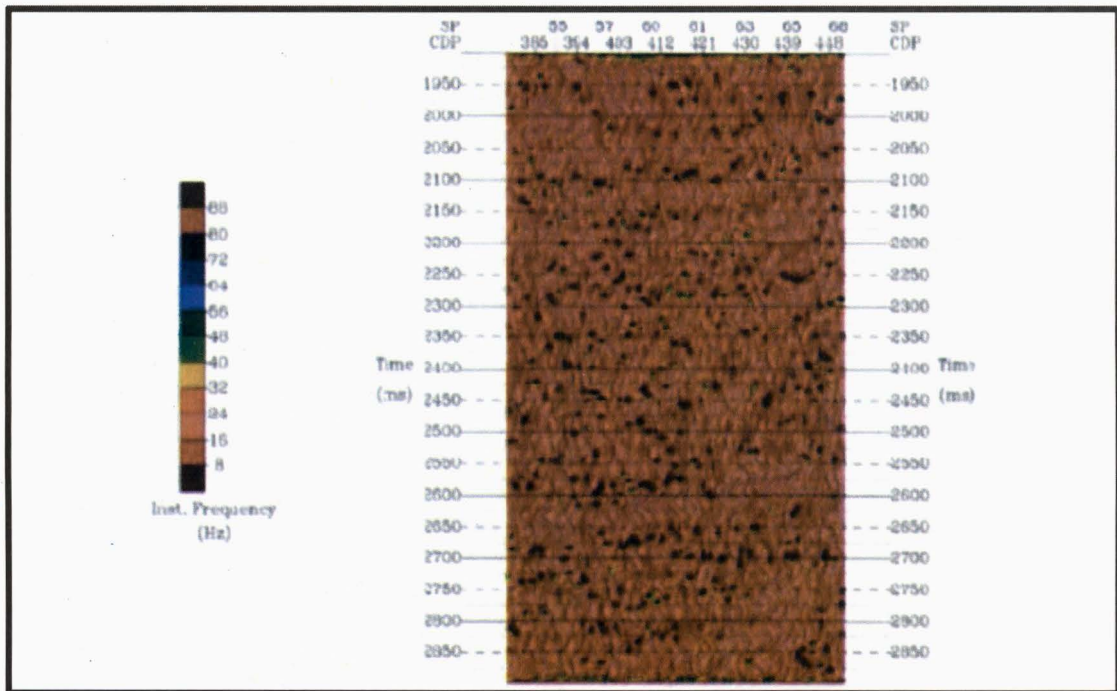


Fig. 8 - Frequency attribute representation
Représentation en attribut fréquence instantanée

Hydrocarbon accumulations are frequently characterized by a very low frequency zone just below the accumulation, so it is interesting to locate zones of abnormal low frequency changes due to lithology are progressive; those due to hydrocarbon occurrence are more abrupt.

USE OF DIRECT HYDROCARBON INDICATORS (D.H.I)

Compressional and shear wave, fractional velocity variations $\Delta V_p/V_p$ and $\Delta V_s/V_s$ respectively, were widely used in this study as direct hydrocarbon indicators. Introduction of gas in rock pores instead of water affects greatly P wave velocity whereas S wave velocity changes slightly; so, representation in $\Delta V_p/V_p$ in the present of gas will show a drop in amplitude values while representation of the same event in $\Delta V_s/V_s$ shows little changes (fig.9a). By

representing anomaly near CDP 388 at double time 2630ms (fig. 9a) in $\Delta V_p/V_p$ one can show relatively great values of fractional velocity; the same anomaly in $\Delta V_s/V_s$ shows only fluid presence. This may be a result of fluid presence. This anomaly is relatively deep and attributed to Ordovician.

FALSE BRIGHT SPOT EXAMPLE

As above mentioned, bright spots are not always due to gas presence; the following example is very interesting as it shows the difficulty of identifying true bright spots of false bright spots. Anomaly near CDP 810 at double time 1700ms was localised on line A, on intercept x gradient representation (fig. 10). Positive values are visible at top of this layer. Generally, the presence of gas in pores produces positive values (red colour) at top and bottom of the

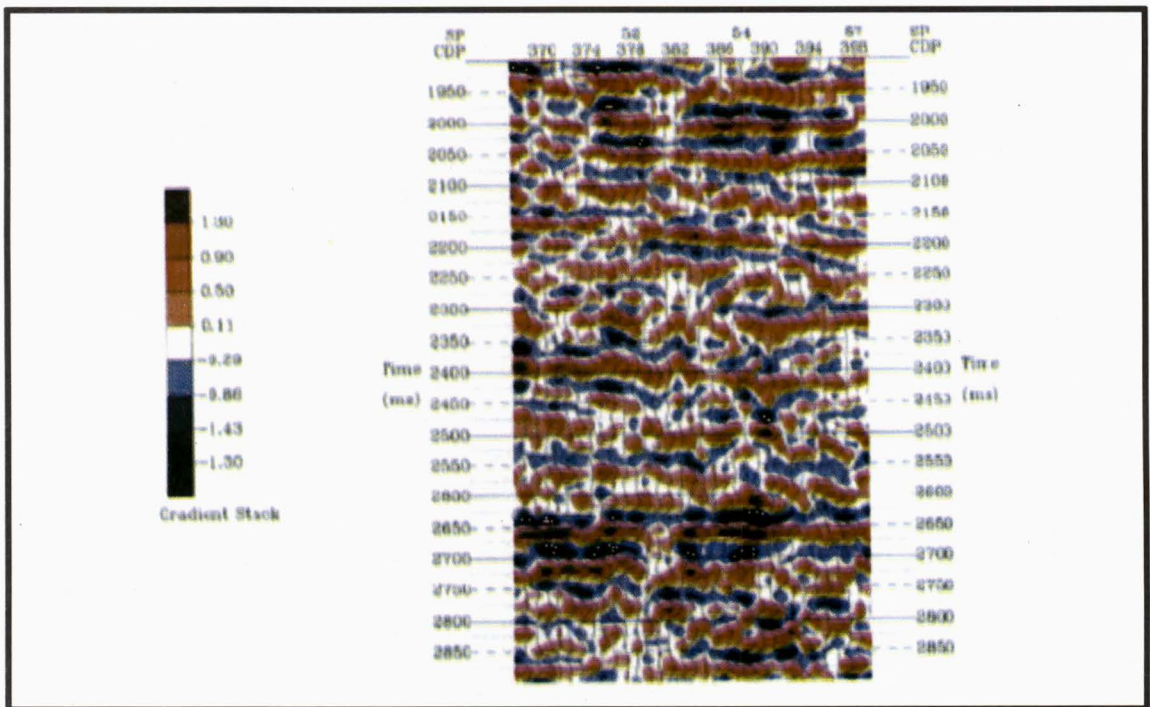


Fig. 9a - $\Delta V_p/V_p$ ratio representation of anomaly at double time 2650ms near CDP 388

Représentation en $\Delta V_p/V_p$ de l'anomalie sise au temps double 2650ms près du CDP 388

CONTRIBUTION OF SEISMIC ATTRIBUTES IN THE DIRECT DETECTION OF HYDROCARBON

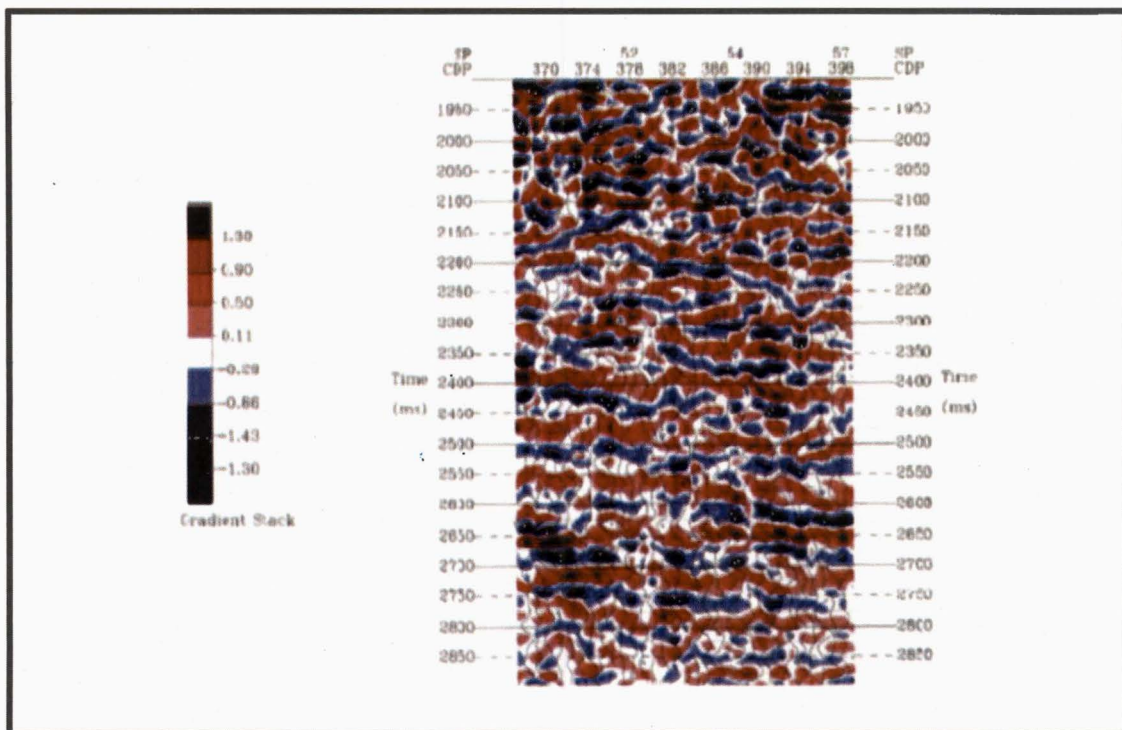


Fig. 9b - $\Delta V_s / V_s$ ratio representation of figure 9a anomaly

Représentation en $\Delta V_s / V_s$ de l'anomalie signalée en figure 9a

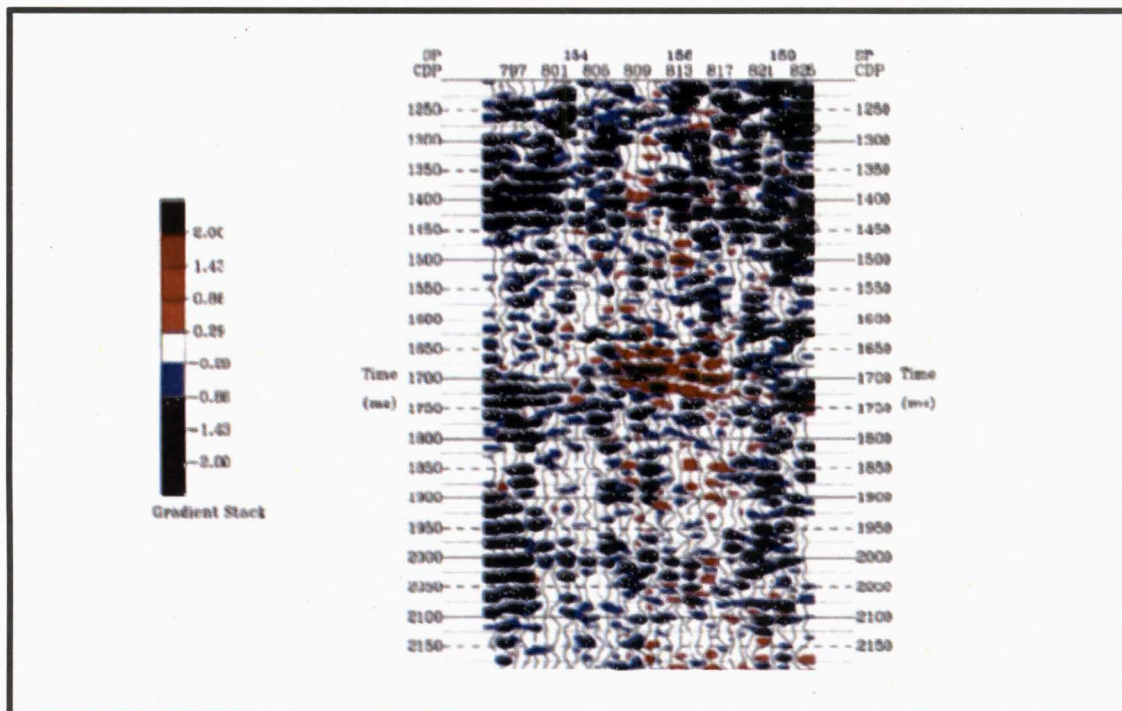


Fig. 10 - P*G representation of anomaly at double time 1700ms near CDP 810

*Représentation P*G pour l'anomalie sise au temps double 1700ms près du CDP 810*

layering intercept x gradient , whereas on fluid factor representation, only bottom is positive (red colour), top is negative (blue colour); this does not appear in figure 11 where the top is positive and bottom is negative and that is probably due to a compressional velocity increase. Figure 12 is coofset representation ; as we can see, there is an increase in peaks, positive values at double time 1680ms whereas gas produces an increase in negative values. We have isolated the more negative values of anomaly near CDP 810 (class III anomaly) on AB plane (fig. 13) and by reporting these values on a cross section (fig. 14), we state inversion of top and bottom positions. After checking logs we have established that anomaly near CDP 810 was due to a very high velocity anhydrite formation, so our assumption about this anomaly was founded.

CONCLUSION

This study has confirmed that the use of seismic attributes is very efficient in fluid detection in structural formations as faults for example. Data used in this study were of high noise ratio and low fold coverage made our work very difficult. We recommended parabolic Radon transform in noise suppression. We showed that seismic attributes are efficient , it is nevertheless the case that amplitude is the most powerful attribute. False bright spot example has proved that we should not make hastily interpretations and *a priori* geological informations are of great help.

In this study we recommended a detailed study at CDPs 580 to 680 on line B; these are here the anomaly of a structure already crossed by well-5, in particular CDP 688.; most of these

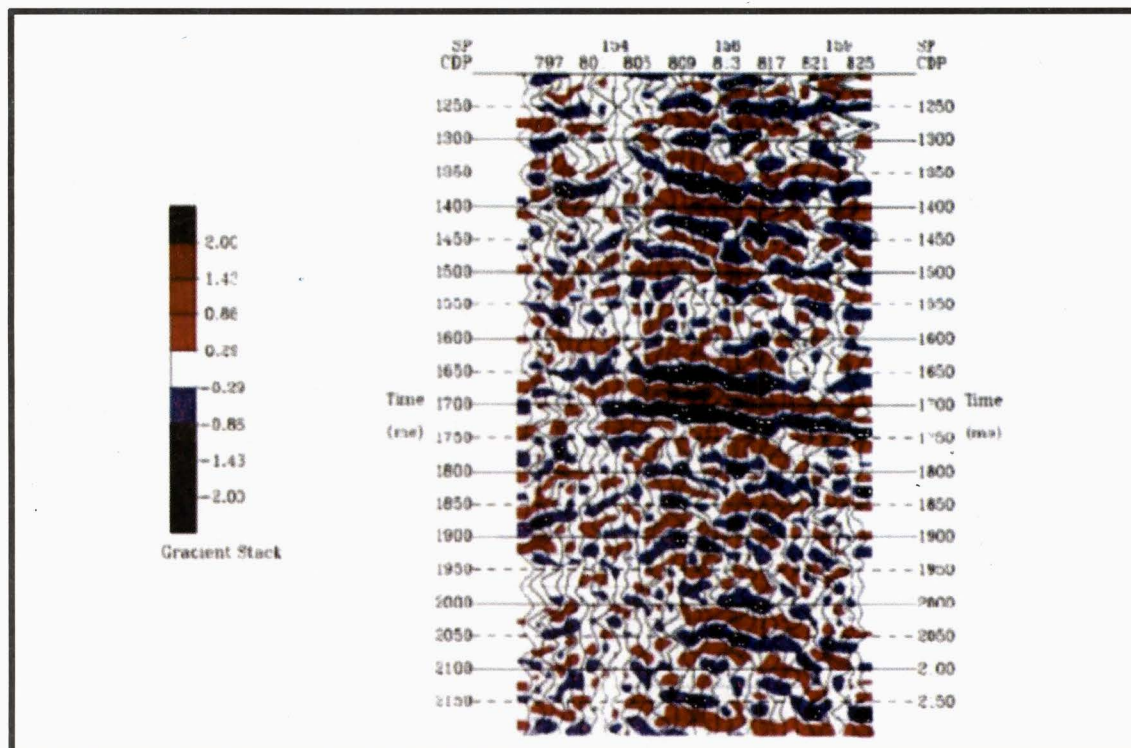


Fig. 11 - Fluid factor representation of figure 10 anomaly
 Représentation en facteur fluide de l'anomalie signalée en figure 10

CONTRIBUTION OF SEISMIC ATTRIBUTES IN THE DIRECT DETECTION OF HYDROCARBON

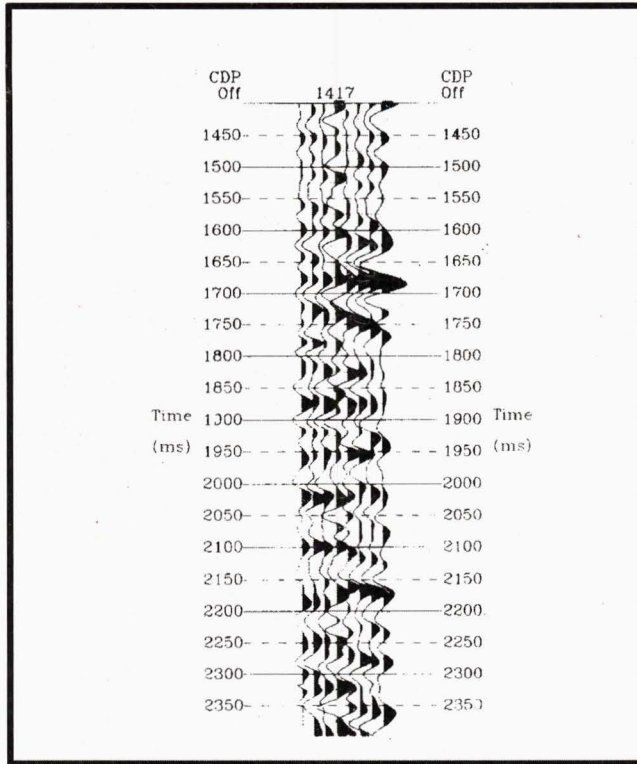


Fig. 12 - Cooffset representation of anomaly seen on figure 10
 Représentation co-offset de l'anomalie signalée en figure 10

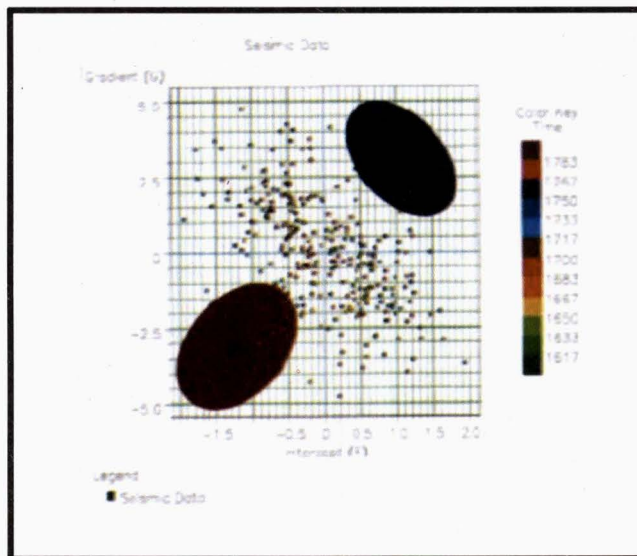


Fig. 13 - AB plane analysis of anomalous zone
 Analyse dans le plan AB de la zone d'anomalie

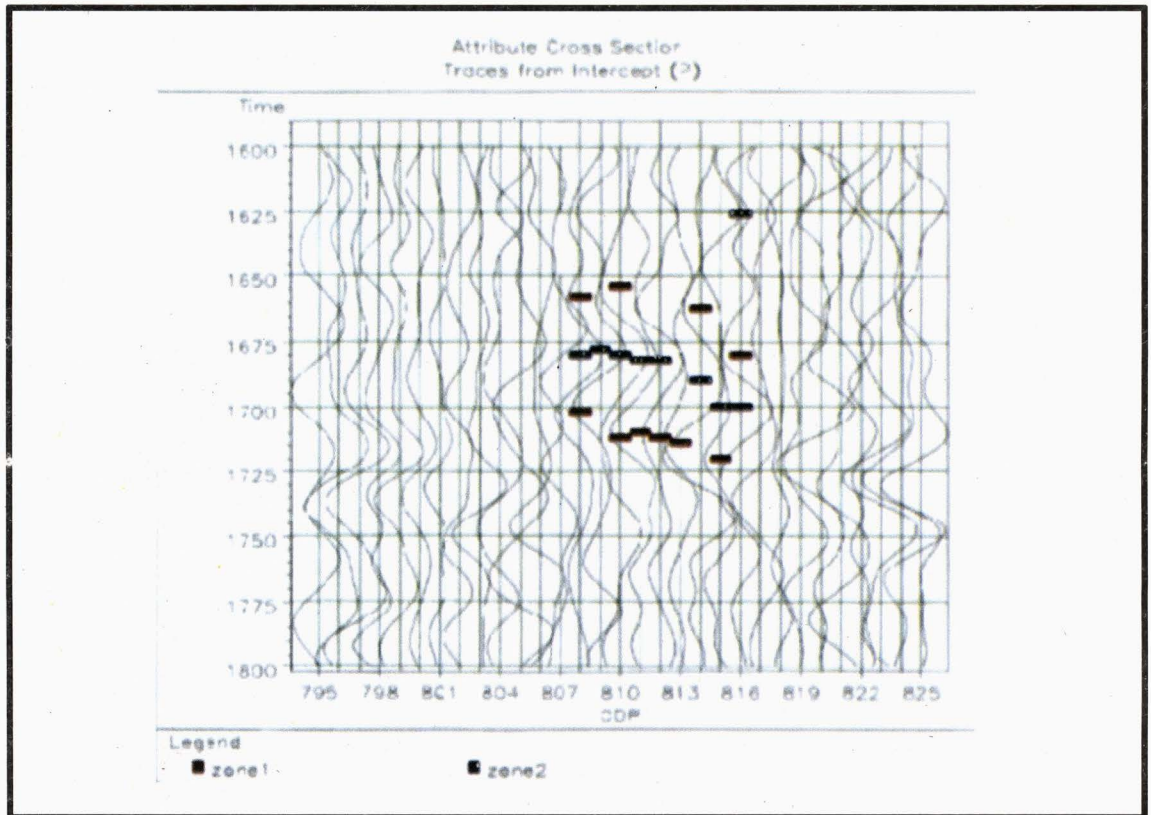


Fig. 14 - Anomalous zone points projection on cross section

Points de projection de la zone d'anomalie en cross-section

anomalies are located at TAGS, TAGI and Gothlandian. Finally, we recommended the use of high fold coverage, 3D data, in the future.

Acknowledgments - We are very grateful to SONATRACH and ENAGEO for their authorization of using their data, as to Mr. Bouberak for his precious help.

REFERENCES

- BOGGS, Jr. S., 1995.** Principle of sedimentology and stratigraphy (second edition). *Printice Hall New-York.*
- BROWN, A.R., 1987.** The value of seismic amplitude, the Leading Edge of *Exploration* 6, 30-33.
- CASTAGNA, J.P. AND BACKUS, N.M., 1994.** Offset dependent reflectivity: theory and practice of AVO analysis. *Library of Congress USA.*
- DJEDDI, MBRK. ET BADDARI, K., 1994.** Eléments de sismologie. *OPU Alger.*
- HENRY, G., 1994.** Géophysique des bassins sédimentaires. *Technip France.*
- HILTERMAN, F. AND SEBAR, M., 2000.** Seismic acquisition with large offset. *Seismic Market Hart's.*
- JAMES, D.R. AND HENRI, H.N., 1984.** Complex seismic traces analysis of thin beds. *Geophysic* 49-344-352.
- JONES, T. D., 1986.** Pore fluid and frequency dependent wave propagation in rocks: *Geophysics* 51 1939-1953.
- KASSOURI, A. DJEDDI, M. AND DJEDDI Mbrk., 2002.** Variation des amplitudes des ondes sismiques avec la distance émetteur-récepteur – application pour la détection du gaz. *Bul. du Serv. Géol. de l'Alg.* vol. 13 n° 2 Juillet 2002.

- KASSOURI, A., BACHTA, M., AND DJEDDI, M., 2000.** 6-8 Nov second symposium. Geology of Northwest Lybia Tripoli Multi component seismic design and innovations.
- OSTRANDER, W.J., 1984.** plane wave reflection coefficient for gas sands at non normal angles incidence *Geophysics* 62, 713-722.
- RÜGER, A., 1997.** P-wave reflection coefficients for transversally isotropic models with vertical and horizontal axis of symmetry. *Geophysics* 62 713-722
- SELLAM, R., DJEDDI, Mbrk. and CHOUAKI, A., 2000.** 6-8 Nov second symposium Geology of Northwest Lybia Tripoli Multi component seismic design and innovations
- SMITH, G.C. AND SUTHERLAND, R. A., 1996.** the fluid factor as an AVO indicator *Geophysics* 61 1425-1428.
- SHUEY, R. T., 1985.** A simplification of the Toeplitz equations. *Geophysics* 50 PP 509-614.
- SHERIF, R.E. AND TANER, M. T., 1979.** Seismic attributes help define reservoirs *Oil and Gas Journal* 182-186.
- JAMES, D. R., HENRI, H.N., 1984.** Complex seismic trace analysis of thin beds. *Geophysics* 49 – 344-352.
- HILTERMAN, F. SEBAR, M., 2000.** Seismic acquisition with large offset *Seismic Market Hart's E et P* 103-106.